19. Huang SC, Barrio JR, Yu DC, et al. Modelling approach for separating blood time-activity curves in positron emission tomographic studies. *Phys Med Biol* 1991;36:749–761.
20. Landaw EM, DiStephano JJ. Multiexponential, multicompartmental, and noncompartmental modeling. II. Data analysis and statistical considerations. *Am J Physiol* 1984;246:R655–R677.
21. Chan GLY, Hewitt KA, Pate BD, Schofield P, Adam MJ, Ruth TJ. Routine determination of [^{18}F]-L-6-fluorodopa and its metabolites in blood plasma is essential for accurate positron emission tomography studies. *Life Sciences* 1991; 50:309–318.
22. Huang SC, Barrio JR, Hoffman JM, et al. A compartmental model for 6-[F-18]fluoro-L-DOPA kinetics in cerebral tissues [Abstract]. *J Nucl Med* 1989;30:735.
23. Gjedde A, Reith J, Dyve S, et al. Dopa decarboxylase activity of the living human brain. *Proc Natl Acad Sci* 1991;88:2721–2725.

Evaluation of Lung Ventilation and Alveolar Permeability in Cirrhosis

Chia-Hung Kao, Chih-Kua Huang, Shih-Chuan Tsai, Shyh-Jen Wang and Gran-Hum Chen
Department of Nuclear Medicine and Division of Gastroenterology, Taichung Veterans General Hospital, Taiwan, Republic of China

This study sought to evaluate lung ventilation and alveolar permeability (AP) in patients with cirrhosis of the liver. **Methods:** Pulmonary function in 29 patients with cirrhosis was measured by ^{99m}Tc-DTPA aerosol inhalation lung scintigraphy, using commercial lung radioaerosol delivery units. Equilibrium lung ventilation images were visually interpreted according to the presence or absence of inhomogeneous distribution, inverted base-to-apex gradient and segmental defects. Degree of AP damage to the upper, middle, lower and total right lung was expressed as the slopes of the time-activity curves from dynamic lung images. The patients were classified into three groups, according to cirrhotic severity, using the modified Child's classification (A = good; B = fair; C = poor). Twelve healthy nonsmokers (2 women, 10 men; 42–75 yr old) formed the control group, and all had normal chest radiographic and pulmonary function test results. **Results:** None of the 29 patients had significantly abnormal lung ventilation findings, but 13 had reduced lung ventilation in the basilar lung zone. The incidence of lung ventilation abnormalities was 20% (3 of 15), 50% (3 of 6) and 88% (7 of 8) in patients with nil, slight-to-moderate and moderate-to-severe ascites, respectively ($p < 0.05$ for nil versus moderate-to-severe ascites). The AP studies showed higher time-activity curve slopes for patients with cirrhosis than for normal control subjects. The slopes for the right total lung showed no significant differences among the three groups; however, those for right upper and right lower lung showed significant differences between some subgroups. In addition, albumin and bilirubin levels showed no significant correlation with slope values in cirrhotic patients. **Conclusion:** Although lung ventilation is normal in most patients with cirrhosis of the liver (16 [55%] of 29 in the present study), the disease can predispose patients to AP damage; however, the degree of damage is not related to cirrhotic severity.

Key Words: cirrhosis; lung ventilation; alveolar permeability
J Nucl Med 1996; 37:437–441

Impairment of pulmonary function has long been associated with severe hepatic disease (*1,2*); however, the physiological mechanism of impairment has not been completely elucidated. In recent years there has been an increase in the use of ^{99m}Tc-DTPA radioaerosols for clinical investigations. Aerosols have replaced radioactive gases, such as ^{81m}Kr and ^{133}Xe, at some centers. Technetium-99m-DTPA radioaerosols, generated by a jet nebulizer, are inexpensive, readily available and have good scintigraphic quality. Technetium-99m-DTPA radioaerosols have been used to visualize lung ventilation (*3–5*) and to evaluate alveolar permeability (AP) (*6–10*) in various diseases. The present study sought to evaluate ^{99m}Tc-DTPA radioaerosol lung scintigraphic changes in lung ventilation and AP in patients with cirrhosis of the liver.

Received Jan. 11, 1995; revision accepted Jun. 17, 1995.
For correspondence or reprints contact: Chia-Hung Kao, MD, Department of Nuclear Medicine, Taichung Veterans General Hospital, 160 Taichung Harbor Road, Section 3, Taichung 40705, Taiwan, Republic of China.

MATERIALS AND METHODS

Patients

Twenty-nine patients (3 women, 26 men; aged 36–75 yr) with cirrhosis of the liver secondary to chronic hepatitis were included in the study. The patients were classified into three groups according to severity of liver cirrhosis, using the modified Child's classification, which takes into account encephalopathy, ascites, bilirubin and albumin levels, prothrombin index and prothrombin time: class A = good; class B = fair; class C = poor (*11*). The AP of patients with cirrhosis was compared with that of 12 normal control subjects (2 women, 10 men; 42–75 yr old). No control subject had a history of smoking, and all chest radiographic findings and pulmonary function test results were normal (Table 1).

Radioaerosol Inhalation Lung Scintigraphy

Technetium-99m was chelated to DTPA by introducing 50 mCi pertechnetate into a vial containing 20 mg DTPA and 2.2 mg tin chloride. Technetium-99m-DTPA was prepared no more than 1 hr before use, and ^{99m}Tc-DTPA radioaerosol was generated by a commercial lung aerosol delivery unit that contained 20 mCi ^{99m}Tc-DTPA in 2 ml saline. Radioaerosol droplet size was measured by an inertial impactor. The mass median aerodynamic diameter of the ^{99m}Tc-DTPA radioaerosol was smaller than 1 μm, with an oxygen air flow rate of 7 liters/min. All subjects were studied in the supine position, and they inhaled for 2 min from the aerosol delivery unit until the total radioactivity was more than 200,000 counts by normal tidal breathing. Data were collected for another 30 min by means of a large-field computerized gamma camera over the posterior view that included the entire chest. The data were acquired as a series of 30 consecutive frames of 1-min duration each in a 64 × 64 matrix with word mode.

Data Analysis

Lung Ventilation. After background correction, the first image in the series was selected as the equilibrium lung ventilation image. Two independent observers judged the lung ventilation images according to established criteria (*12,13*), which included the presence or absence of inhomogeneous distribution, inverted base-to-apex gradient, segmental defects and basilar hypoventilation.

TABLE 1
Clinical Characteristics, Washout Rates and LV during Technetium-99m-DTPA Aerosol Ventilation Scintigraphy in Control Subjects

Subject no.	Sex	Age (yr)	Height (cm)	Weight (kg)	Washout rate (%/min)				LV
					RUL	RML	RLL	RTL	
1	M	69	161	62	0.11	0.68	1.83	0.88	Normal
2	M	42	160	68	0.75	0.47	0.72	0.76	Normal
3	M	63	176	77	0.53	1.28	1.32	1.21	Normal
4	F	68	158	55	0.31	0.67	1.95	0.93	Normal
5	M	75	170	68	0.80	1.36	2.09	1.43	Normal
6	M	62	168	63	1.28	0.92	2.22	1.25	Normal
7	M	66	175	70	1.37	1.64	0.95	1.41	Normal
8	M	63	169	68	0.53	1.28	1.32	1.21	Normal
9	M	58	173	75	0.42	1.02	0.45	0.64	Normal
10	M	64	165	61	0.37	1.21	0.26	0.53	Normal
11	F	64	155	56	0.25	0.31	0.56	0.54	Normal
12	M	62	165	68	0.61	0.66	0.67	0.76	Normal

RUL = right upper lung; RML = right middle lung; RLL = right lower lung; RTL = right total lung; LV = lung ventilation.

Alveolar Permeability. The summation of the series of 30 images was displayed. Four regions of interest (ROIs) were manually created over the upper, middle, lower and total right lung. Radioactivity was corrected for radionuclide decay, and background-corrected time-activity curves (Fig. 1) were generated individually for the upper, middle and lower third portion and the total right lung. An exponential line of best fit was calculated for each ROI. The negative slope of this regression line was designated as the washout rate and was expressed as percent decrease in radioactivity per minute (%/min). The right lung was selected for analysis of radioactivity clearance to avoid possible higher background radioactivity from the stomach due to swallowed ^{99m}Tc-DTPA radioaerosols just below the left lung.

RESULTS

Clinical characteristics and lung ventilation and AP data for the 29 study patients are shown in Table 2. No patient had significant lung ventilation abnormalities, such as inhomogeneous distribution, inverted base-to-apex gradient or segmental defects; however, 13 (45%) had an abnormal lung ventilation pattern with reduced lung ventilation in the basilar lung zone (Fig. 2). The Fisher's exact test was used to analyze the differences in abnormal lung ventilation among the three patient groups, and the statistical results are shown in Table 3. Table 3 also shows the incidence of basilar hypoventilation for the three groups: 29% (4 of 14), 50% (5 of 10) and 80% (4 of 5 for classes A, B and C, respectively). These results show mild statistical significance ($0.5 > p > 0.05$) among the three patient groups.

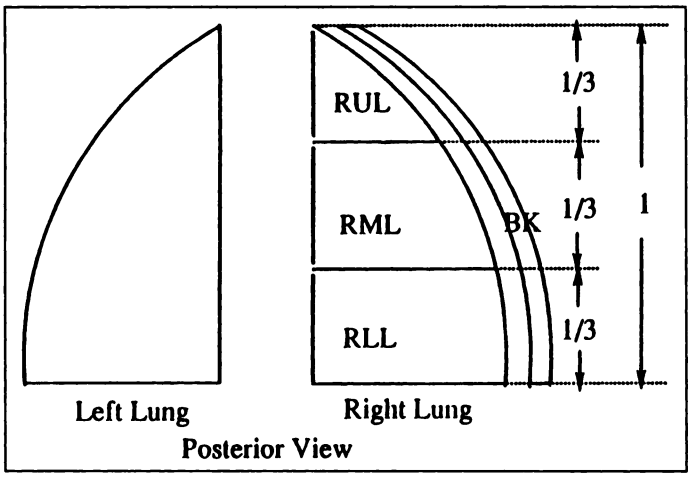

FIGURE 1. Method of choosing ROIs in regions of the right lung and selected area of background (BK) correction. The BK correction formula is as follows: Corrected mean counts/pixel in ROIs = Original mean counts/pixel in ROIs − Mean count/pixel in BK area. RUL = right upper lung; RML = right middle lung; RLL = right left lung.

The Fisher's exact test was also used to analyze the differences in the incidence of abnormal lung ventilation among the three patient groups according to severity of ascites, and the statistical results are shown in Table 4. Table 4 also shows the incidence of abnormal lung ventilation for the three groups: 20% (3 of 15), 50% (3 of 6) and 88% (7 of 8) for nil, slight to moderate and moderate to severe ascites, respectively). These results show statistical significance ($p < 0.05$) for nil versus moderate to severe ascites.

Table 5 shows the washout rates of ^{99m}Tc-DTPA. The Student's and Mann-Whitney U-tests were used to analyze the differences between normal control subjects and patients with cirrhosis, and the statistical results are shown in Table 6. Although the difference is not very significant ($p = 0.13$), patients with cirrhosis had a higher mean slope value (1.21 ± 0.51 %/min) than normal control subjects (0.96 ± 0.33 %/min). The differences in slopes for right total lung among the three groups (1.16 ± 0.46, 1.28 ± 0.67, 1.21 ± 0.33 %/min for classes A, B and C, respectively) are not statistically significant ($p = 0.62–0.84 > 0.5$). However, significant differences ($p < 0.05$) were seen for control subjects versus patients with cirrhosis, control subjects versus patients in class A and control subjects versus patients in class B for right upper lung; and for control subjects versus patients in class C for right lower lung.

In addition, the correlation coefficient, expressed as R^2 values of serum albumin and bilirubin versus slope values for patients with cirrhosis, was not significant ($R^2 = 0.037$ and 0.013).

DISCUSSION

The lung parenchyma is essentially a three-compartment structure, comprising the alveolar space, the vascular space and the interstitium. The integrity of these compartments is fundamental to the maintenance of normal gas exchange. Small aerosols can move across the compartments through transcellular and intercellular route compartments (*14,15*). The ^{99m}Tc-DTPA radioaerosol inhalation lung scan is a sensitive marker of the changes in permeability characteristics of the lung parenchyma. Technetium-99m-DTPA is deposited in the lining layer

TABLE 2
Clinical Characteristics, Washout Rates and Lung Ventilation Status during Technetium-99m-DTPA Aerosol Ventilation Scintigraphy in Patients with Liver Cirrhosis

Patient no.	Sex	Age (yr)	Washout rate (%/min) RUL	RML	RLL	RTL	Lung Ventilation	Ascites	Albumin (g/dl)	Bilirubin (mg/dl)
1	F	54	0.07	0.57	2.22	0.76	Abnormal	MS	2.0	7.1
2	M	36	0.43	1.22	0.94	0.99	Abnormal	MS	2.4	31.4
3	M	61	1.43	1.61	2.88	1.56	Abnormal	MS	1.7	4.2
4	M	64	1.93	1.26	3.05	1.41	Abnormal	MS	1.9	4.9
5	M	64	1.08	1.17	2.16	1.32	Normal	N	0.7	4.5
6	M	68	2.91	2.60	2.56	2.62	Abnormal	MS	1.5	2.4
7	F	55	0.72	1.14	1.05	0.43	Abnormal	SM	3.8	1.5
8	M	60	1.88	1.99	1.90	1.94	Abnormal	MS	3.6	1.6
9	M	62	1.56	1.68	2.82	0.99	Abnormal	SM	2.7	1.0
10	M	70	0.32	0.40	0.37	0.83	Abnormal	SM	2.1	2.8
11	F	64	1.06	1.26	1.70	1.15	Normal	MS	2.8	2.5
12	M	66	1.57	1.70	0.70	1.88	Normal	SM	3.1	2.4
13	M	60	0.96	1.11	2.21	0.77	Normal	SM	2.3	4.9
14	M	64	0.68	0.35	1.23	1.21	Normal	N	4.4	1.6
15	M	75	0.80	0.97	3.50	0.95	Normal	SM	3.7	1.2
16	M	66	1.52	1.39	1.92	1.41	Abnormal	N	3.4	0.6
17	M	67	1.86	1.15	1.43	1.12	Abnormal	N	2.8	2.4
18	M	60	0.84	0.67	0.83	0.85	Abnormal	N	3.2	1.4
19	M	59	1.25	1.08	0.60	0.97	Abnormal	MS	3.1	1.1
20	M	66	2.32	1.53	1.80	1.51	Normal	N	4.1	1.1
21	M	67	1.27	0.94	1.36	0.22	Normal	N	3.2	1.0
22	M	54	1.76	1.72	1.25	0.85	Normal	N	4.8	2.0
23	M	62	1.40	1.40	1.39	1.45	Normal	N	3.9	1.4
24	M	64	0.20	0.27	1.61	2.01	Normal	N	3.6	2.4
25	M	55	0.62	0.40	0.04	0.86	Normal	N	4.8	0.8
26	M	65	0.91	1.16	0.54	1.44	Normal	N	3.6	1.6
27	M	61	3.44	2.13	1.38	1.73	Normal	N	4.2	0.6
28	M	69	0.49	0.65	1.47	0.87	Normal	N	3.9	1.3
29	M	55	1.25	0.83	0.77	0.98	Normal	N	3.6	2.4

RUL = right upper lung; RML = right middle lung; RLL = right lower lung; RTL = right total lung; MS = moderate to severe; N = nil; SM = slight to moderate.

of the pulmonary epithelial surface and then passes through the barrier (*16*). Under these conditions, enhanced epithelial permeability occurs early and appears to be a very sensitive index of pulmonary damage (*17*). The ^{99m}Tc-DTPA radioaerosol lung scan has been used to investigate epithelial permeability under different physiological conditions (*7,8*) in subjects who smoke (*18*) and in patients with various pulmonary disorders (*6,19*). Clearance of ^{99m}Tc-DTPA increases in patients with diseases known to involve the alveolar-capillary membrane, such as adult respiratory distress syndrome (*19*) and interstital lung disease (*6*).

Multiple factors, such as radioaerosol molecular weight, deposition site, recirculation, stability, ventilation pattern, exercise and posture, can affect AP (*7,14,17,20*). Comparison of our normal reference values with our previously published data (*21,22*) was very difficult and nearly impossible. In general, the normal washout rate in the supine position for younger, healthy nonsmokers is approximately 0.8–0.9 %/min (*21,22*). This rate seems slightly faster than ours (0.96 %/min), which may be due to the use of a different procedure.

Since the publication of Child's classification (*23*), there has been success in estimating the severity of liver disease. Because the Child's classification includes measures of liver function (serum bilirubin, serum albumin, prothrombin time) and severity of ascites, we consider it adequate for representing cirrhotic severity in the present study.

Pulmonary function has been studied in patients with cirrhosis of the liver (*1*). The results show no impairment of air distribution and no inequality of ventilation (*1*). Although

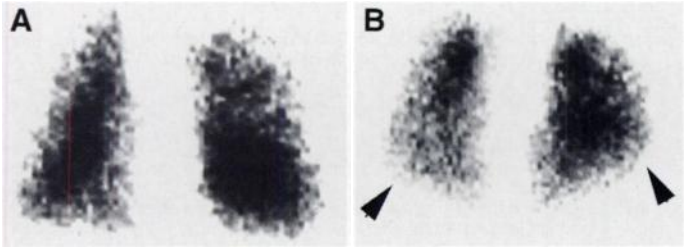

FIGURE 2. Normal (A) and abnormal (B) lung ventilation patterns. Reduced ventilation is seen in basilar zone of right lung (arrow).

TABLE 3
Incidence of Abnormal Lung Ventilation during Technetium-99m-DTPA Aerosol Ventilation Scintigraphy in Subjects and Patients

Study group	Incidence of abnormal lung ventilation (no. of pts)	p value	
Control subjects	0% (0/12)	<0.02	
Patients with cirrhosis	45% (13/29)		
Class A	29% (4/14)	0.26	
Class B	50% (5/10)		0.07
Class C	80% (4/5)	0.29	

Class A = good; Class B = fair; Class C = poor.

TABLE 4
Incidence of Abnormal Lung Ventilation during Technetium-99m-DTPA Aerosol Ventilation Scintigraphy in Cirrhotic Patients According to Severity of Ascites

Severity of ascites	Incidence of abnormal lung ventilation (no. of pts)	p value	
N	20% (3/15)	0.20	<0.05
SM	50% (3/6)		
MS	88% (7/8)	0.18	

N = nil; SM = slight-to-moderate; MS = moderate-to-severe.

measurements with ^{133}Xe showed reduced ventilation in the basilar lung zones in cirrhotic patients without ascites (*24*), in our study the results of lung ventilation with ^{99m}Tc-DTPA radioaerosols revealed that massive ascites may cause lung ventilation of the basilar lung zone in patients with cirrhosis (Table 4).

Davis et al. (*2*) concluded that hepatic cirrhosis predisposes some patients to dilated gas-exchanging blood vessels. Berthelot et al. (*25*) reported that in 13 patients with cirrhosis, the alveolar septa of the lungs were more vascular than that of normal subjects (*25*). Previous studies (*24,26–28*) have concluded that biliary cirrhosis in rats and humans leads to dilated small pulmonary vessels and increased vascular permeability. The clearance of small aerosols from the alveoli is primarily limited by diffusion (*14,29–31*), and the diffusion rate is related to regional pulmonary blood flow (*29–31*) and AP.

TABLE 5
Washout Rate of Technetium-99m-DTPA in Subjects and Patients

Study group	Washout rate (%/min)			
	RUL	RML	RLL	RTL
Control subjects	0.61 ± 0.39	0.96 ± 0.41	1.20 ± 0.69	0.96 ± 0.33
Patients with cirrhosis	1.26 ± 0.77	1.18 ± 0.56	1.58 ± 0.85	1.21 ± 0.51
Class A	1.37 ± 0.83	1.09 ± 0.52	1.17 ± 0.54	1.16 ± 0.46
Class B	1.25 ± 0.76	1.32 ± 0.70	1.80 ± 0.99	1.28 ± 0.67
Class C	0.99 ± 0.75	1.17 ± 0.38	2.25 ± 0.83	1.21 ± 0.33

RUL = right upper lung; RML = right middle lung; RLL = right lower lung; RTL = right total lung; Class A = good; Class B = fair; Class C = poor.

TABLE 6
Student's and Mann-Whitney U-Test Analysis of Differences in Control Subjects and Patients

Classification	p values			
	RUL	RML	RLL	RTL
Controls vs. cirrhosis	<0.05	0.21	0.18	0.13
Controls vs. class A	<0.05	0.47	0.92	0.22
Controls vs. class B	<0.05	0.14	0.11	0.16
Controls vs. class C	0.19	0.34	<0.05	0.18
Class A vs. class B	0.72	0.37	<0.05	0.62
Class A vs. class C	0.38	0.78	<0.05	0.84
Class B vs. class C	0.54	0.66	0.40	0.83

RUL = right upper lung; RML = right middle lung; RLL = right lower lung; RTL = right total lung; cirrhosis = patients with cirrhosis of the liver; class A = good; class B = fair; class C = poor.

The clearance of small hydrophilic aerosols such as ^{99m}Tc-DTPA depends on both capillary permeability and regional perfusion (*7,8,32,33*). The increased vascularity and capillary permeability of the alveoli result in increased blood flow and permeability and are most likely responsible for the increase in clearance of ^{99m}Tc-DTPA radioaerosols (a larger slope value) in our study. In addition, changes in the structure of the aerohematic barrier were found in mice with liver cirrhosis, and these changes are similar to those found in interstitial lung disease (*34*). Changes in aerohematic barrier structure may also play a role in the increased rate of alveolar clearance of ^{99m}Tc-DTPA radioaerosols in cirrhotic patients.

CONCLUSION

Cirrhosis of the liver can predispose patients to basilar hypoventilation and mild AP damage; however, the degree of AP damage is not related to cirrhotic severity. The presence of basilar hypoventilation and AP damage may represent the initial signs of lung complications in patients with cirrhosis and may be considered an alternative to traditional diagnostic tools, such as chest radiographs and pulmonary function tests.

ACKNOWLEDGMENTS

Supported in part by a grant from the National Council of Science, Taiwan, Republic of China.

REFERENCES

1. Schomerus H, Buchta I, Arndt H. Pulmonary function studies and oxygen transfer in patients with liver cirrhosis and different degree of portasystemic encephalopathy. *Respiration* 1975;32:1–20.
2. Davis HH II, Schwartz DJ, Lefrak SS, Susman N, Schainker BA. Alveolar-capillary oxygen disequilibrium in hepatic cirrhosis. *Chest* 1978;73:507–511.
3. Alderson PO, Biello DR, Gottschalk A, et al. Technetium-99m-DTPA aerosol and radioactive gases compared as adjuncts to perfusion scintigraphy in patients with suspected pulmonary embolism. *Radiology* 1984;153:515–521.
4. Miller RF, Jarritt PH, Lui D, Kidery J, Semple SJG, Ell PJ. The APE nebulizer—a new delivery system for the alveolar targeting of particulate technetium-99m diethylene triamine penta-acetic acid. *Eur J Nucl Med* 1991;18:164–170.
5. Selby JB Sr, Gardner JJ. Clinical experience with technetium-99m-DTPA aerosol with perfusion scintigraphy in suspected pulmonary embolism. *Clin Nucl Med* 1987;12:1–5.
6. Rinderknecht J, Shapiro L, Krauthammer M, et al. Accelerated clearance of small solutes from the lungs in interstitial lung disease. *Am Rev Respir Dis* 1980;121:105–117.
7. Meignan M, Rosso J, Leveau J, et al. Exercise increases the lung clearance of inhaled technetium-99m-DTPA. *J Nucl Med* 1986;27:274–280.
8. Meignan M, Rosso J, Robert R. Lung epithelial permeability to aerosolized solutes: relation to position. *J Appl Physiol* 1987;62:902–911.
9. Mason GR, Ulzer JM, Effros RM, Reid E. Rapid reversible alteration of pulmonary epithelium permeability induced by smoking. *Chest* 1983;83:6–11.
10. Rosso J, Guillon JM, Parrot A, et al. Technetium-99m-DTPA aerosol and gallium-67 scanning in pulmonary complications of human immunodeficiency virus infection. *J Nucl Med* 1992;33:81–87.
11. Dimagno EP, Zinsmeister AR, Larson DE, et al. Influence of hepatic reserve and cause of esophageal varices on survival and rebleeding before and after the introduction of sclerotherapy: a retrospective analysis. *Mayo Clin Proc* 1985;60:149–157.
12. Pulera N, Santolicandro A, Bernard P, Solfanelli S, Giuntini C. Monodisphere labeled aerosol to visualize airflow redistribution in the lung after a mucokinetics drug. *J Nucl Med Allied Sci* 1989;33:258–263.
13. Taplin GV, Tashkin DP, Chopra SK, et al. Early detection of chronic obstructive pulmonary disease using radionuclide lung-imaging procedures. *Chest* 1977;71:567–575.
14. Dolovich MB, Jordana M, Newhouse MT. Methodologic considerations in mucociliary clearance and lung epithelial absorption measurements. *Eur J Nucl Med* 1987;13:S45–S52.
15. Newhouse MI, Jordana M, Dolovich M. Evaluation of lung epithelium permeability. *Eur J Nucl Med* 1987;13:S58–S62.
16. Parker JC, Falgout HJ, Parker RE, Granger N, Taylor AE. The effect of fluid volume loading on exclusion of interstitial albumin and lymph flow in the dog lung. *Circ Res* 1979;45:440–450.
17. Todisco T, Dottorini M, Rossi F, Baldoncini A, Palumbo R. Normal reference values for regional pulmonary peripheral airspace epithelial permeability. *Respiration* 1989; 55:84–93.
18. Mason GR, Ulzer JM, Effros RM, Reid E. Rapid reversible alteration of pulmonary epithelium permeability induced by smoking. *Chest* 1983;83:6–11.

19. Jones JG, Royston D, Minty BD. Changes in alveolar-capillary barrier function in animals and humans. *Am Rev Respir Dis* 1983;127:S51–S59.
20. Dusser DJ, Minty BD, Collignon MG, Hinge D, Barritault LG, Huchon GJ. Regional respiratory clearance of aerosolized ^{99m}Tc-DTPA: posture and smoking effects. *J Appl Physiol* 1986;60:2000–2006.
21. Smith RJ, Hyde RW, Waldman DL, et al. Effect of pattern of aerosol inhalation on clearance of technetium-99m-labeled diethylenetriamine pentaacetic acid from the lungs of normal humans. *Am Rev Respir Dis* 1992;145:1109–1116.
22. Groth S, Hermansen F, Rossing N. Pulmonary permeability in never-smokers between 21 and 67 yr of age. *J Appl Physiol* 1989;67:422–428.
23. Child CG III, Turcotte CG. Surgery and portal hypertension. In: Child CG III, ed. *The liver and portal hypertension*. Philadelphia: WB Saunders; 1964:50.
24. Spagnolo SV. Cyanosis of cirrhosis. *Med Clin North Am* 1975;59:983–987.
25. Berthelot P, Walker JG, Sherlock S, Reid L. Arterial changes in the lungs in cirrhosis of the liver—lung spider nevi. *N Engl J Med* 1966;274:291–298.
26. Ohara N, Voelkel NF, Chang SW. Tissue eicosanoids and vascular permeability in rats with chronic biliary obstruction. *Hepatology* 1993;18:111–118.
27. Chang SW, Ohara N. Increased pulmonary vascular permeability in rats with biliary cirrhosis: role of thromboxane A2. *Am J Physiol* 1993;264:L245–L252.
28. Kuroyanagi T, Kura K. A new method for evaluating an increased general capillary permeability in patients. *Tohoku J Exp Med* 1977;122:331–336.
29. Guyton AC. Physical principles of gaseous exchange; diffusion of oxygen and carbon dioxide through the respiratory membrane. In: Guyton AC, ed. *Textbook of medical physiology*, 8th ed. Philadelphia: W.B. Saunders; 1991:422–432.
30. West JB. Uptake and delivery of the respiratory gases. In: West JB, ed. *Best and Taylor's physiological basis of medical practice*, 11th ed. Baltimore: Williams & Wilkins; 1985:546–571.
31. Mines AH. Gas exchange in the lungs. In: Mines AH, ed. *Respiratory physiology*, 2nd ed. New York: Raven Press; 1986:103–128.
32. Rizk N, Luce J, Hoeffel J, et al. Site of deposition and factors affecting clearance of aerosolized solute from canine lungs. *J Appl Physiol* 1984;56:723–729.
33. Braude S, Royston D, Coe C, Barnes P. Histamine increases lung permeability by an H2-receptor mechanism. *Lancet* 1984;18:372–374.
34. Alekseevskikh IUG. State of the air-blood barrier in experimental liver cirrhosis. *Arkh Patol* 1982;44:36–42.

Whole-Body PET: Physiological and Artifactual Fluorodeoxyglucose Accumulations

Hermann Engel, Hans Steinert, Alfred Buck, Thomas Berthold, Rahel A. Huch Böni and Gustav K. von Schulthess
Divisions of Nuclear Medicine and Diagnostic Radiology, Department of Medical Radiology, University Hospital, Zürich, Switzerland

The purpose of this study was to semiquantitatively identify artifactual and physiological soft-tissue accumulations in whole-body FDG-PET scans with the aim of defining their frequency and anatomic distribution. **Methods:** Fifty whole-body FDG-PET scans performed for the staging of malignant melanoma were obtained from transaxial scans and reconstructed without absorption correction by filtered backprojection in the form of coronal and sagittal sections. The patients were asked to stay n.p.o. for at least 4 hr and interrogated about their physical activity prior to injection and until scanning. Classification of FDG organ accumulations was done using grades 0–6. Means and standard deviations on this scale were then calculated for multiple organs and muscle groups and tabulated. **Results:** On this grading scale, viscera showed uptake grades between 1.7 ± 0.5 and 2.05 ± 1.0. Except for the intestines, the activity in these organs was homogeneously distributed. Relatively high average uptake values of 2.0–4.2 (s.d. ≥ 2.3) were found in various muscle groups, especially the orbital musculature. Myocardial uptake was visible in 90% of the scans. Reconstruction artifacts were seen around the renal collecting system and the bladder. **Conclusion:** Most of the "normal" accumulations of FDG in nonattenuation corrected whole-body PET are readily recognized and distinct from the usually focal FDG accumulation associated with metastatic disease, but the diagnostician must be familiar with them. Muscular FDG uptake is related to physical activity prior and immediately following injection and can be minimized by proper patient instructions and positioning.

Key Words: PET; fluorine-18-FDG; physiological accumulations

J Nucl Med 1996; 37:441–446

With the introduction of PET scanners with high detection efficiency and a large axial field of view of 15 cm or more, whole-body PET with [^{18}F]fluorodeoxyglucose (FDG) has become a clinical reality. Typically, axial scan distances of 150 cm can be covered in 60 min (two-dimensional mode) and substantial improvement in acquisition time can be expected from the introduction of three-dimensional data acquisition protocols. The result of such whole-body data acquisition is a set of 450 or more transaxial slices that can be reformatted into coronal and sagittal planes at will (Fig. 1). Several studies have documented PET as a sensitive method for tumor staging because FDG preferentially accumulates in many types of malignant tumor cells (*1–8*) and has well recognized physiological accumulation sites (*4,5,9–12*).

When reading whole-body PET scans, it is important to distinguish physiological and artifactual FDG accumulations from those that are pathological (*1,4*), as normal findings have to be distinguished from those that are abnormal in any imaging method. In this study, we analyzed the occurrence and appearance of such "normal" activity accumulations in nonattenuation-corrected whole-body FDG-PET scans by looking at a multitude of organ sites.

MATERIALS AND METHODS

Patients

Fifty whole-body PET scans were obtained in patients referred for tumor staging of malignant melanoma. The patients (30 men, 20 women) ranged in age from 18 to 80 yr. Patients with diabetes mellitus were excluded because of their pathologic glucose metabolism which affects FDG uptake in an uncontrolled fashion unless glucose clamping is used (*13*). All patients participating in this study consented to having a PET scan. Each patient was questioned about their physical activities in the period preceeding FDG injection and whether they had been comfortable during the phase between injection and scanning and the PET examination itself.

PET

The patients were explicitly asked to stay n.p.o. for at least 4 hr prior to the study. Thirty to 40 min prior to scanning, the patients received an intravenous injection of 220–370 MBq [^{18}F]FDG while lying on a stretcher in a silent room. FDG was produced at the Paul Scherrer Institute (Villigen, Switzerland) using well

Received Jan. 24, 1995; revision accepted Jun. 29, 1995.
For correspondence or reprints contact: Gustav K. von Schulthess, MD, PhD, Division of Nuclear Medicine, Department of Medical Radiology, University Hospital, CH-8091 Zürich, Switzerland.